Proceedings of the 10th World Congress on Mechanical, Chemical, and Material Engineering (MCM'24)
Barcelona, Spain - August 22-24, 2024
Paper No. ICMIE 112
DOI: 10.11159/icmie24.112

An influence of flux components in A-TIG welding of copper Cu-ETP sheets

Matija Bušić[1], Sanja Šolić[1], Vlado Tropša[1] and Damjan Klobčar[2]
[1] Department of Mechanical Engineering, University North
Jurja Križanića 31b, 42000 Varaždin, Croatia
mbusic@unin.hr (M.B.); ssolic@unin.hr (S.Š.); vtropsa@unin.hr (V.T.)
[2]Faculty of Mechanical Engineering, University of Ljubljana
Aškerčeva 6, 1000 Ljubljana, Slovenia
damjan.klobcar@fs.uni-lj.sipaper

Abstract **–** Tungsten inert gas (TIG) welding of copper is concerned difficult because of its high coefficient of thermal expansion and high thermal conductivity. Activated TIG welding (A-TIG) has been investigated and verified successful as a welding method for obtaining deeper penetration on various metals. However, A-TIG welding of copper remains unexplored without known influence of flux substances, applied parameters and achieved mechanical properties in produced welds. Three substances were examined as single component fluxes in this experiment: Calcium oxide (CaO), Silicon dioxide (SiO_2) and Sodium carbonate (Na_2CO_3). Produced welds were characterized by visual inspection and macrostructural analysis, also bend testing and tensile strength testing were conducted. Microstructure of the weld with optimal mechanical properties was analyzed by means of Field Emission Gun-Scanning Electron Microscope (FEG-SEM) and also the chemical characterization of the weld was made by means of Energy Dispersive Spectroscopy (EDS). The results showed that the most effective flux used was Silicon dioxide. Welds welded with SiO_2 showed good results in visual inspection, macrostructure analysis and band test and also have acceptable values of tensile strength. However, oxide inclusions have been found in weld metal in significant percentage which could indicate the possible degradation of electrical conductivity of the material.

Keywords**:** A-TIG welding, Cu-ETP, Activating flux, Silicon dioxide

1. Introduction

Copper is reddish, soft, malleable and ductile metal, one of the few metals that can occur in nature in a directly usable metallic form. It is widely applied in many industrial applications playing a key role in the generation, delivery and use of electricity. From high voltage transmission wire and microcircuits to gigawatt generators and computers, copper is vital to every aspect of electricity generation, transmission and use. Copper and copper alloys have high electrical and thermal conductivities, good combinations of strength and ductility, processability using different production technologies and excellent corrosion resistance [1-4]. The electrical conductivity depends on chemical composition, the level of cold deformation and the grain size. Cu-ETP copper is an electrolytically refined, oxygen-containing copper. The high oxygen content in tough pitch copper can lead to embitterment in the heat affected zone and weld metal porosity.

Welding of copper alloys can be performed using Manual Metal Arc welding (MMA), Tungsten Inert Gas welding (TIG), Metal Inert Gas welding (MIG), Plasma Arc Welding (PAW) and Submerged Arc Welding (SAW) [5, 6]. Other welding processes involving sophisticated equipment as Laser Beam Welding, hybrid Laser – MIG welding and Friction Stir Welding (FSW) have been researched and successfully applied [7-10]. For welding copper or copper alloys the suitable type of current and shielding gas must be selected to provide maximum welding heat input that can supplements the fast heat dissipation through the material and cooling of the weld zone. Preheating is recommended for welding thicker sections of copper alloys. Recommended temperature in degrees Celsius can be calculated by multiplying the thickness of sheets (mm) by 100 considering upper limit may not exceed 600 °C.

TIG welding is widely applied technology for joining copper or copper alloys. Material thickness greater than 3 mm is necessary to weld in multiple passes and this greatly reduces productivity. Helium or a mixture of helium and argon is recommended as shielding gas for automated welding of thin sections and for manual welding of thicker sections [5]. Activated TIG welding (A-TIG) is a welding technology developed for increasing the penetration depth of the electric arc using standard equipment for TIG welding. It is based on application of a thin coating of activating flux material onto the workpiece surface prior to welding. Activating flux usually consists of single or mixture of oxides (CaO, Cu_2O, NiO, Cr_2O_3,

SiO_2, MnO_2, V_2O_5, ZnO, KCr_2O_7, TiO, TiO_2, Ti_2O_3, Fe_2O_3, Al_2O_3, aluminium, selenium or sulphur) and halides (CaF_2, MgF_2, $MgCl_2$, Na_2WO_4, AlF_3 or CdCl) [11-19].

There are many different theories defining how activating flux effects the TIG process. For A-TIG welding of steel, Makara et al. used fluxes which give off vapours of fluorides, chlorides, oxygen compounds and other elements [16]. It was concluded that the ability of the flux to wet the surface of the weld pool had an effect on the surface tension which lead to deeper penetration. Simonik et al. proposed a theory of effectiveness of a flux content in constricting electric arc and linked it to a higher temperature of molecule formation and ionisation potential [13]. The conclusion was that the halogen entering the arc will be discharged either as neutral atom, as molecules, and as positive or negative ions. Along the axis of arc discharge the most probable state is a neutral atomic state with an extremely small quantity of positively charged ions. The ionization potential is the potential difference that is just sufficient to ionize a gas molecule or to remove an electron completely from the atom. The energy equivalent to ionization potential is called ionization energy. Due to the high value of ionization energy, there is hardly any ionization of the halogen atoms and all the processes are determined by elements of lower ionisation potential [13].

A-TIG welding has been investigated and confirmed successful in getting deeper welds in various metals including carbon steels [15, 17], stainless steels [11, 16], Incoloy [20] and magnesium alloys [14]. Only a research from Rana et. [21] reports about A-TIG welding of copper alloys. They have investigated the influences of single component fluxes on the depth to width ratio during welding of oxygen free copper with A-TIG. The fluxes which outperformed with all techniques were MoO_3 and MgO. The conclusion in this work was that the flux agents constrict the electric arc reversing Marangoni effect. It is important to point out that ionization potential of Mo is 6.8 eV which is slightly below ionization potential of Cu (7.5 eV) and much below the Ar (15.2 eV) and He (23.7 eV). However, it is found that influence of the fluxes containing other agents could be investigated and the mechanical properties of produced weld should be measured. The principal idea in this experiment was to use fluxes with elements that have ionization potential near to that of Cu and far below the ionization potential of used shielding gas. Substances used as single component fluxes in this work: Calcium oxide (CaO), Silicon dioxide (SiO_2) and Sodium carbonate (Na_2CO_3) have ionization potentials 5.8, 7.8 and 4.9 eV respectively.

2. Materials and methods

The specimens for this research were prepared from Cu-ETP sheets with dimensions 190 × 75 × 3 mm and containing 99.9 % Cu. According to technical specification, copper sheets used in this work have tensile strength R_m = 248.9 MPa. However, Cu-ETP sheets usually soften when exposed to raised temperature for the certain time resulting in a significant loss of strength in the heat affected zones. This softening occurs at temperatures above 150 °C which is normally exceeded in welding processes. Hardness can decrease up to 50 % [22].

Each flux used in this work was prepared with 30 g of single component powder (CaO, SiO_2 and Na_2CO_3) mixed in 40 ml of ethanol to provide coating attachment on the surface of sheets in width of 15 mm. Welding was performed in butt joint configuration from one side without backing, using VARTIG 2005 AC/DC welding machine with automatic guidance system. Used shielding gas was helium/argon mixture with components share 50:50 with a gas flow 20 l/min. Welding parameters for all samples are presented in table 1. Variable parameters in welding process were welding speed v, cm/min and current I, A. These parameters along with voltage U, V combine welding heat input Q, kJ/cm as the main parameter. After the welding the samples were visually inspected. According to penetration on the root side, on the entire length of the weld, it was decided that the flux composed of SiO_2 has provided the best results. As a consequence, this flux was applied more times with different heat inputs for obtaining more experimental conditions. After welding test specimens were sectioned for bend tests, tensile strength testing, microstructure analysis and the microchemical characterization with the EDS. The specimens in dimensions 20 × 10 × 3 mm were prepared for microstructure analysis using the standard metallography procedure for welded specimens and analysed using stereomicroscope equipped with CANON EOS 200d digital camera. Dimensions of the weld were measured using ImageJ image processing software.

Table 1. Welding parameters

Weld designation	Flux type	*I*, A	*U*, V	*V*, cm/min	*Q*, kJ/cm
W1	-	165	16.6	20	4.93
W2	CaO	165	16.6	20	4.93
W3	SiO_2	135	15.4	20	3.74
W4	SiO_2	145	15.8	22	3.75
W5	SiO_2	145	15.8	24	3.43
W6	SiO_2	145	15.8	26	3.17
W7	SiO_2	150	15.9	20	4.29
W8	Na_2CO_3	155	16.2	22	4.11

Bend test was performed according to the standard ISO 5173:2009 [23] to confirm absence of imperfections on or near the surface of the welded joint. Four specimens were prepared from each produced weld, except specimen W8 which was immediately eliminated because of complete absence of welding. Two specimens were prepared for transverse face bend test and the other two for transverse root bend test. Testing samples were in dimensions 150 × 15 × 3 mm.

Tensile strength testing was performed on specimens extracted from the welds that have passed visual inspection, macrostructure analysis and bend testing (welds W4, W5, W6 and W7). From each produced weld two specimens were machined and labeled accordingly (for the weld W5 specimens are W5.1 and W5.2). Original cross-sectional area of the parallel part was S_O = 30 mm^2 and the parallel length was L_C = 50 mm. The uniaxial tensile testing was conducted with constant stress control according to ISO 6892-1 [24] and with constant speed of applied load 12 MP/a.

Microstuctural analysis was performed on specimen sectioned from weld W5 by means of Thermo Scientific Quattro S FEG SEM. Secondary electrons were used for imaging, while the chemical quantitative microanalysis was done by EDS using Oxford Instruments Ultim Max 65 Energy-dispersive Detector with Aztec software. The analysis included observation of the specimen morphology to detect possible presence of microcracks and flux agent inclusions in weld metal.

3. Results

Fig. 1 shows visual appearance of produced welds. Lack of penetration can clearly be seen on the root side of welds W1, W2 and W8 testing specimen and after first half of weld W3. Narrow weld width and incomplete penetration can also be observed on weld W6 after good start and proper weld geometry.

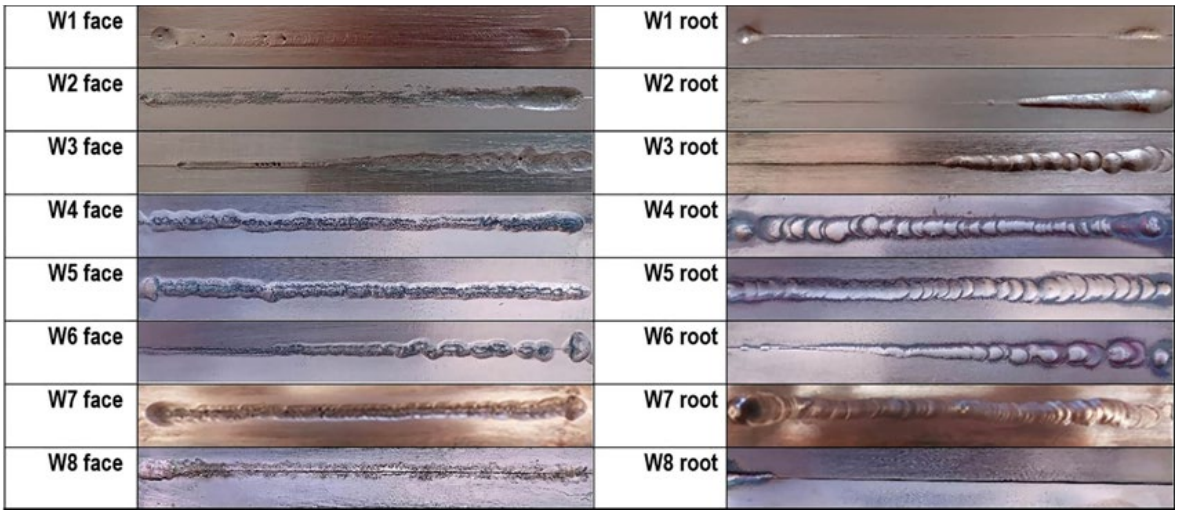

Figure 1: Visual appearance of produced welds.

Fig. 2 presents cross sections of produced welds with measured weld width on face and root side. As specimens where sectioned 20 mm from the welding starting point specimens sectioned from welds W2 and W3 have full penetration although it reduces after. There were no inclusions or porosity observed in all produced welds presented in Fig. 2.

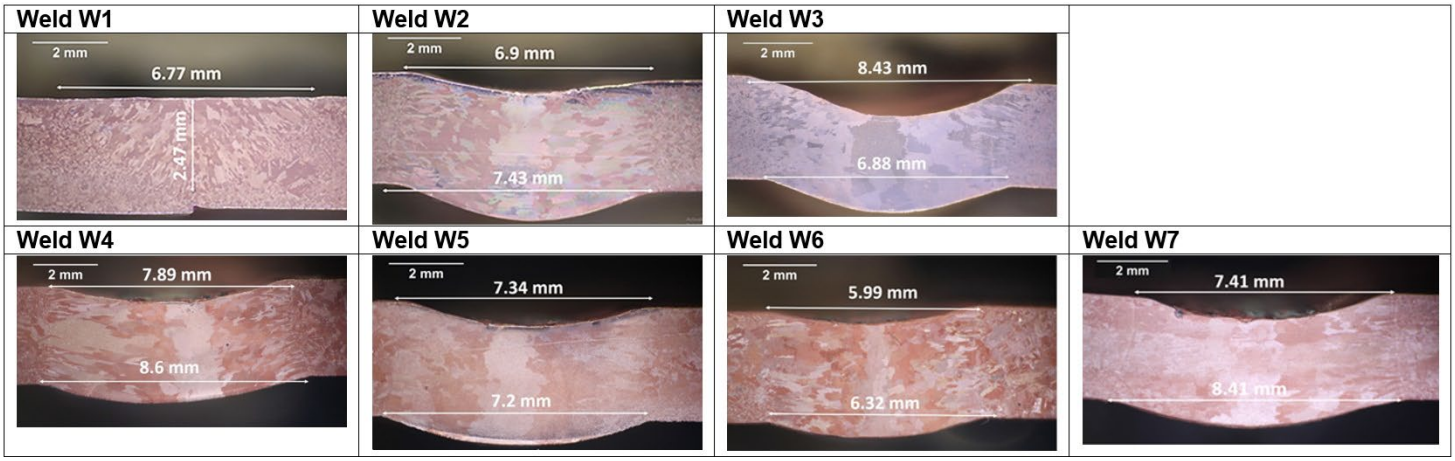

Figure 2: Cross sections of produced welds

Figs. 3 and 4 present specimens after transverse bend test of butt welds. These specimens have been completely bent around the former. The visual inspection of the bent specimens showed that specimens presented in Fig. 3 have failed and specimens in Fig. 4 have passed the bend test.

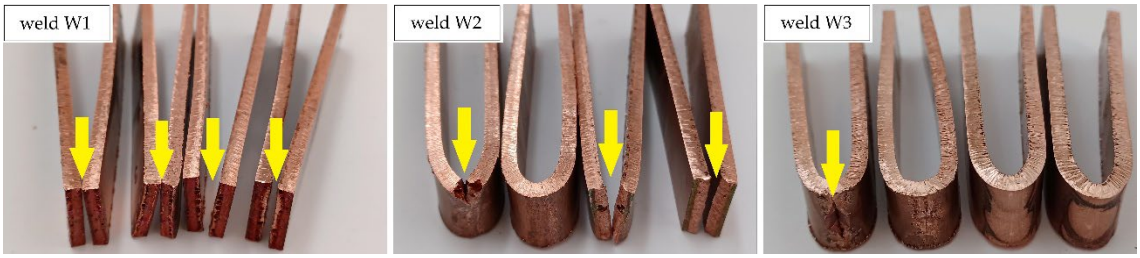

Figure 3: Specimens sectioned from welds W1, W2 and W3 after transverse bend test.

Figure 4: Specimens sectioned from welds W4 – W7 after transverse bend test.

Tensile strength testing results are presented in Table 2. Testing was performed only on specimens extracted from the welds W4 - W7 that have passed visual inspection and bend testing. The mean value of tensile strength $\overline{R_m}$, MPa for each weld was calculated from results by two specimens. The lowest value of tensile strength was measured on specimen extracted from W5. To identify the reasons for the lowest tensile strength, macrostructural specimen from weld W5 was chosen for further microstructural analysis and the microchemical characterization with the EDS. Figs. 5 and 6 present SEM

micrographs of weld metal from weld W5. Three locations of EDS chemical microanalysis have been marked in Fig. 6. The corresponding results of this analysis are presented in Table 3.

Table 2: Tensile strength testing results

Weld desig.	F_{max} , kN	R_m, Mpa	$\overline{R_m}$, Mpa
W4 .1	5.31	180.78	174.53
W4 .2	4.95	168.27	
W5.1	5.12	174.20	174.19
W5.2	5.15	175.22	
W6.1	4.99	169.82	190.73
W6.2	6.22	211.64	
W7.1	5.94	188.7	183.3
W7.2	5.04	177.99	

Table 3: EDS chemical microanalysis results in weld W5

elements	Spectrum 1	Spectrum 2	Spectrum 3
O	2.90	4.36	-
Si	-	0.95	-
Cu	97.10	94.69	100.00
Total	100.00	100.00	100.00

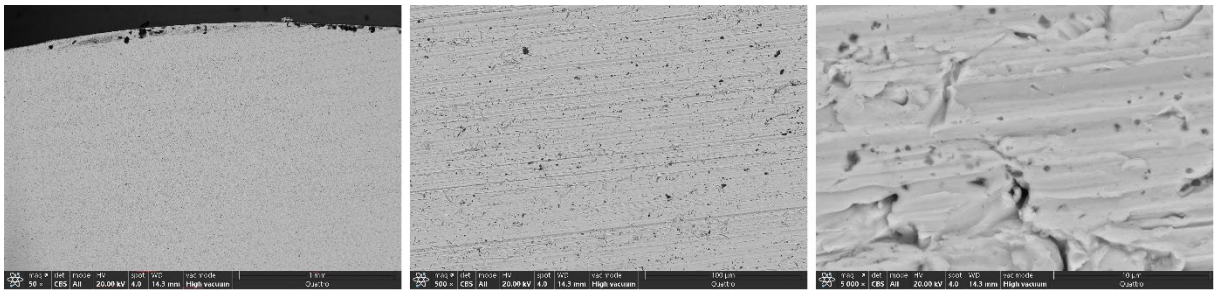

Figure 5: SEM micrographs of weld metal in weld W5 with magnification from left to right: 50×, 100× and 5000×.

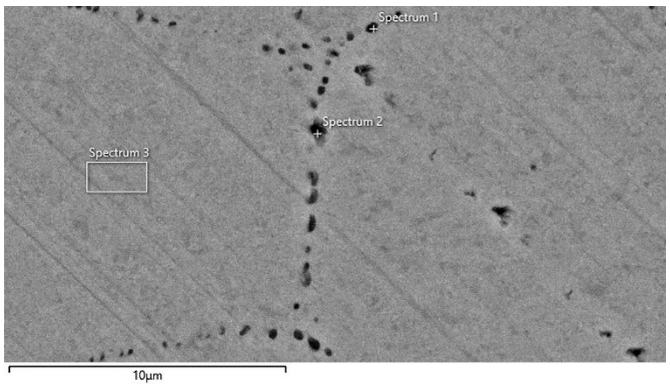

Figure 6: SEM micrograph of weld metal in weld W5 with marked locations of EDS chemical microanalysis.

4. Discussion

Although weld W1 has been TIG welded without flux with highest heat input (4.93 kJ/cm) the weld penetration was not adequate. This can be observed in Fig. 1 and confirmed with bend testing results (Fig. 3). In weld W1 the heat input was not sufficient for obtaining full penetration. Welds welded using different fluxes for A-TIG welding show significantly different results. Visual inspection of the samples presented in Fig. 1 clearly show that flux composed of Na_2CO_3 used for welding of testing specimen W8 is completely inappropriate and harmful for weld surface and A-TIG welding. CaO flux on specimen W2 has increased the weld penetration at a start of the weld. However, heat input was insufficient to counteract high thermal conductivity and heat dissipation. The prediction is that with higher heat input it will be possible to supplements the fast head dissipation through the material and cooling from the localized weld zone. This thoroughly depends on strong influence of parameters variations in TIG welding of copper as it is presented in literature from other authors [4–6].

Welds W3 – W7 have shown positive influence of flux containing SiO_2 on the weld penetration and a melting profile accomplished with arc constriction. Welds W4, W5 and W7 have complete penetration in full length although they were welded with less heat input when compared to weld W1. When heat input is lower the weld bead is decreased (Fig. 2). The influence of flux mixing method and manual application of the flux coating on the surfaces is noticeable in weld tortuosity. Despite straight electrode guidance by automatic guidance system, accumulation of SiO_2 particles in some places resulted with uneven melting process stability and irregular surface on the face and bottom sides of the welds W3-W7 as presented in Fig. 1. It is worth noting that the samples processed with A-TIG demonstrated larger grains in the middle and long needle-shaped grains at the boundary of fusion zone and heat affected zone. The same structure is observed in the work of Rana et al. [21]. Fusion zone of A-TIG experienced rapid heating which is followed by rapid cooling due to high thermal conductivity of the copper, thus instigating directional solidification towards heat affected zone which decelerates the grain growth and defines their orientation.

Bend testing was performed in order to assess ductility and confirm absence of imperfections on or near the surface of the welded joint. Welds W1, W2 and W3 have failed the bending test because samples have been completely broken at the root or even on the face side. Welds W4 - W7 have passed bend testing which confirmed absence of kissing bonds, lack of fusion or brittle structures (Fig. 4). Tensile strength tests presented fairly uniform results. Welds W4, W5 and W7 are very similar in weld geometry and also similar results have been measured in tensile strength testing. As it has been mentioned before, strength can fall for 50 % in heat affected zone of cold worked copper sheets. In this experiment welds with proper weld geometry have the strength around 174 MPa that is 70 % of strength of the base material.

SEM micrographs of weld metal in Fig. 5 and Fig. 6 have confirmed absence of micro porosities larger than 10 μm, thus confirming a homogeneous structure. Larger porosities have also been excluded in macrostructure analysis (Fig. 2). The structure is composed of alpha copper grains. Eutectic copper and copper oxide Cu_2O can be seen on grain boundaries in Fig. 6. As the solidification of copper is rapid process, oxygen molecules could be entrapped between grains and form micro porosity. Copper dissolves small amounts of oxygen in solid solution (alpha). If the solubility of oxygen is exceeded, eutectic alpha copper and copper oxide Cu_2O are formed, in the weld metal. With EDS chemical microanalysis of specific marked locations (presented in Fig. 6) 2.9 % and 4.36 % of oxide has been measured. The presence of oxide inclusions is also reported in the work of Rana et al. [21]. In A-TIG welding process decomposition of the oxide based flux during welding with high temperature of electric arc may be the reason of oxide presence in the weld metal. Oxides dissolved into the molten pool could escape out, through the surface, during the process of solidification or stay entrapped in the weld metal. These inclusions could reduce the tensile strength and act as crack nucleus especially in application of dynamic loading on the welded joint. Silicon inclusions have been detected in one location in weld metal of specimen W5 in quantity of 0.95 %. Silicon inclusions are present in small percentage and should not have the influence on degradation of weld metal mechanical properties.

The specimens in this work were prepared from Cu-ETP sheets in which a level of 0.02 %–0.04 % oxygen is maintained for oxidation of the remaining impurities to oxides which would otherwise dissolve in the copper forming solid solutions, thereby reducing conductivity. Impurities and oxide inclusions discovered by EDS chemical microanalysis in welded specimens in this work could also decrease electrical conductivity. This indicates that in future work electrical conductivity of A-TIG welded Cu-ETP sheets should be also investigated in detail.

5. Conclusions

Based on the results presented in this work, the following conclusions can be made:

1. TIG welding of Cu-ETP sheets will require heat input above 4.93 kJ/mm if full penetration and proper weld bead is to be achieved.
2. Na_2CO_3 is not appropriate as a flux component for A-TIG welding of CuETP sheets. It produces inappropriate weld surface and has no influence in increasing penetration depth.
3. Flux composed of CaO has certain potential for usage for A-TIG welding of Cu-ETP sheets, thus more suitable parameters need to be adjusted. It is possible to slightly raise the heat input and to produce weld with continuous weld width and full penetration.

4. Flux composed of SiO_2 has strong influence on weld bead geometry and penetration depth in A-TIG welding of Cu-ETP sheets. Using SiO_2 as flux will have significant advantage, full penetration could be achieved with 30 % less heat input when compared with the standard TIG welding of Cu-ETP sheets.
5. A-TIG welding of Cu-ETP sheets with SiO_2 flux will produce weld with required plasticity and formability to pass the three-point bend test according to standard ISO 5173:2009.
6. A-TIG welding of Cu-ETP sheets with SiO_2 flux will produce weld with acceptable tensile strength that is 70 % of tensile strength of the base material. Penetration will be sufficient and weld metal will be free of pores in the microstructure. However, these welds will have oxide inclusions that could reduce dynamic strength and electrical conductivity.

Acknowledgements

This research was funded by: University North support for scientific research and artistic work in 2020 - UNIN-TEH-20-1-14 and University North support for scientific research and artistic work in 2024 – UNIN-TEH-24-1-19. This work was also supported by the Slovenian Research Agency, under grant number P2-0270.

References

[1] O. Cakır, H. Temel, M. Kiyak, "Chemical etching of Cu-ETP copper", *Journal of Materials Processing Technology*, vol. 162-163, pp. 275–279, 2005.
[2] R. N. Caron, R. G. Barth, D. E. Tyler, "Metallography and Microstructures of Copper and Its Alloys - Metallography and Microstructures" in *ASM Handbook*, vol 9, pp. 775–788, 2004.
[3] T. Watari, S. Northey, D. Giurco, S. Hata, R. Yokoi, K. Nansai, K. Nakajima, "Global copper cycles and greenhouse gas emissions in a 1.5 °C world", *Resources, Conservation & Recycling*, vol. 179, pp. 106-118, 2022.
[4] Q. Jiang, P. Zhang, Z. Yu, H. Shi, D. Wu, H. Yan, X. Ye, Q. Lu, Y. Tian, "A Review on Additive Manufacturing of Pure Copper", *Coatings*, vol. 11, no. 6, pp. 760, 2021.
[5] M. N. Rogers, "Welding of Copper Alloys" in Welding brazing and soldering" ed. D. L. Olson, T. A. Siewert, S. Liu, G. R. Edwards, *ASM Handbook*, vol. 6, pp. 1872 -1922, 1993.
[6] D. Raghavendra, B. Vishvesh, M. Kush, J. Jaydeep, Y. Ashish, K. C. Arun, "Investigation on stability of weld morphology, microstructure of processed zones and weld quality assessment for hot wire gas tungsten arc welding of electrolytic tough pitch copper" *Materials and Manufacturing Processes*, vol. 37, no. 8, pp. 908-920, 2020.
[7] S. T. Auwal, S. Ramesh, F. Yusof, S. M. Manladan, "A review on laser beam welding of copper alloys", *The International Journal of Advanced Manufacturing Technology,* vol. 99, pp. 475-490, 2018.
[8] L. J. Zhang, Q. L. Bai, J. Ning, A. Wang, J. N. Yang, X. Q. Yin et al. "A comparative study on the microstructure and properties of copper joint between MIG welding and laser-MIG hybrid welding" *Materials and Design*, vol. 110, pp. 35-50, 2016.
[9] W. B. Lee, S. B. Jung, "The joint properties of copper by friction stir welding", *Materials Letters*, vol. 58, pp. 1041-1046, 2004.
[10] T. Will, T. Jeron, C. Hoelbling, L. Müller, M. Schmidt, "In-process analysis of melt pool fluctuations with scanning optical coherence tomography for laser welding of copper for quality monitoring", *Micromachines*, vol. 13, pp. 1-11, 2022.
[11] D. Klobčar, J. Tušek, M. Bizjak, S. Simončič, V. Lešer, "Active flux tungsten inert gas welding of austenitic stainless steel AISI 304", *Journal Metalurgija*, vol. 55, pp. 617-620, 2016.
[12] C. R. Heiple, J. R. Roper, "Mechanism for minor element effect on GTA fusion zone geometry" *Welding Journal*, vol. 6, no. 4, pp. 97-102, 1982.
[13] A. G. Simonik, V. I. Petviashvili, A. A. Ivanov, "The effect of contraction of the arc discharge upon the introduction of electronegative elements", *Svaroch proizvod,* vol. 23, no. 3, pp. 49-51, 1976.
[14] B. Qin, R. Qu, Y. Xie, S. Liu, "Numerical Simulation and Experimental Study on the TIG (A-TIG) Welding of Dissimilar Magnesium Alloys" *Materials*, vol 15, no. 14, 4922, 2022.

[15] J. Niagaj, “Influence of Activated Fluxes on the Bead Shape of A-TIG Welds on Carbon and Low-Alloy Steels in Comparison with Stainless Steel AISI 304L” *Metals*, vol. 11 no. 4, 530, 2021.
[16] A. M. Makara, B. N. Kushnirenko, V. N. Zamkov, “High-tensile martensitic steels welded by argon tungsten arc process using flux”, *Automatic Welding*, vol. 7, pp. 78-79, 1968.
[17] R. H. Zhang, D. Fan, “Weldability of activating flux in A-TIG welding for mild steel”, *Transactions of the China welding institution*, vol. 1, pp. 85-87, 2003.
[18] P. J. Modenesi, E. R. Apolinario, I. M. Pereira, “TIG welding with single-component fluxes”, *Journal of Materials Processing Technology*, vol. 99, pp. 260-265, 2000.
[19] S. Suman, P. Bashab Chandra, D. Santanu, “Productivity improvement in butt joining of thick stainless steel plates through the usage of activated TIG welding”, *SN Applied Sciences*, vol. 3, a. n. 416, 2021.
[20] S. A. Kumar, P. Sathiya, “Experimental investigation of the A-TIG welding process of Incoloy 800H”, *Materials and Manufacturing Processes*. vol. 30, no. 9, pp. 1154–1159, 2015.
[21] H. Rana, V. Badheka, P. Patel, V. Patel, W. Li, J. Andersson, “Augmentation of weld penetration by flux assisted TIG welding and its distinct variants for oxygen free copper” *Journal of Materials Research and Technology*, vol. 10, pp. 138-151, 2021.
[22] Copper Alliance. European Copper Institute-Cu-ETP, (2023, November 20) [Online]. Available: http://www.conductivity-app.org/alloy-sheet/33 (accessed on 20.11.2023.)
[23] ISO 5173:2009 Destructive tests on welds in metallic materials — Bend tests
[24] ISO 6892-1:2019 Metallic materials — Tensile testing — Part 1: Method of test at room temperature